Cell Chemical Biology, Volume *30*

Supplemental information

HDAC3 and HDAC8 PROTAC dual degrader reveals roles of histone acetylation in gene regulation

Yufeng Xiao, Seth Hale, Nikee Awasthee, Chengcheng Meng, Xuan Zhang, Yi Liu, Haocheng Ding, Zhiguang Huo, Dongwen Lv, Weizhou Zhang, Mei He, Guangrong Zheng, and Daiqing Liao

Supplemental Information

HDAC3 and HDAC8 PROTAC dual degrader reveals roles of histone acetylation in gene regulation

Yufeng Xiao,[1,7] Seth Hale,[2,7] Nikee Awasthee,[2] Chengcheng Meng, [2] Xuan Zhang,[1,8] Yi Liu,[1] Haocheng Ding,[3] Zhiguang Huo,[3] Dongwen Lv,[4,9] Weizhou Zhang,[5] Mei He,[6] Guangrong Zheng,[1]* Daiqing Liao,[2,10*]

*Corresponding Authors

Guangrong Zheng – Department of Medicinal Chemistry, College of Pharmacy, University of Florida, Gainesville, Florida, 32610, United States.

Phone: 352-294-8953; Email: zhengg@cop.ufl.edu

Daiqing Liao – Department of Anatomy and Cell Biology, College of Medicine, University of Florida, Gainesville, Florida, 32610, United States.

Phone: 352-273-8188; Email: dliao@ufl.edu

Authors

Yufeng Xiao – Department of Medicinal Chemistry, College of Pharmacy, University of Florida, Gainesville, Florida, 32610, United States.

Seth Hale – Department of Anatomy and Cell Biology, College of Medicine, University of Florida, Gainesville, Florida, 32610, United States.

Nikee Awasthee – Department of Anatomy and Cell Biology, College of Medicine, University of Florida, Gainesville, Florida, 32610, United States.

Chengcheng Meng – Department of Anatomy and Cell Biology, College of Medicine, University of Florida, Gainesville, Florida, 32610, United States.

Xuan Zhang – Department of Medicinal Chemistry, College of Pharmacy, University of Florida, Gainesville, Florida, 32610, United States.

Current Address: Shanghai institute of Materia Medica, 555 Zuchongzhi Rd, 201203, China.

Yi Liu – Department of Medicinal Chemistry, College of Pharmacy, University of Florida, Gainesville, Florida, 32610, United States.

Haocheng Ding – Department of Biostatistics, College of Medicine, University of Florida, Gainesville, Florida, 32610, United States.

Zhiguang Huo – Department of Biostatistics, College of Medicine, University of Florida, Gainesville, Florida, 32610, United States.

Dongwen Lv – Department of Pharmacodynamics, College of Pharmacy, University of Florida, Gainesville, Florida, 32610, United States.

Current address: Department of Biochemistry and Structural Biology and Center for Innovative Drug Discovery, School of Medicine, University of Texas Health San Antonio, 7703 Floyd Curl Drive, San Antonio, TX 78229, United States

Weizhou Zhang – Department of Pathology, Immunology and Laboratory Medicine, College of Medicine, University of Florida, Gainesville, Florida, 32610, United States.

Mei He – Department of Pharmaceutics, College of Pharmacy, University of Florida, Gainesville, Florida, 32610, United States.

Table S1. The inhibitory activity of modified warheads[a], related to Figure 1

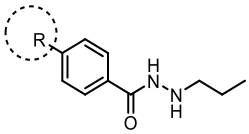

Cpd	R	IC$_{50}$ (nM)[a]		
		HDAC1	HDAC3	HDAC8
13	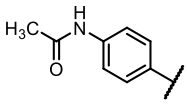	72.0±10.0 [b]	13.0±1.0 [b]	88.2±7.0
14	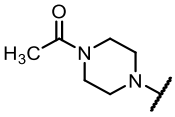	227.4±6.3	28.8±6.5	600.6±124.0
15	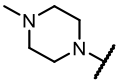	61.4±4.6	10.8±1.2	83.2±2.5
16	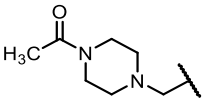	405.6±51.5	793.9±240.6	1,237.5±453.3
17	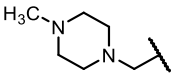	235.1±4.8	188.2±0.6	684.5±54.0
18	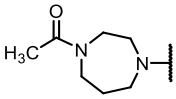	148.0±7.1	53.5±15.6	293.7±56.6
19	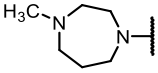	57.4±4.6	17.7±0.8	67.5±7.4
TSA		0.28±0.02	1.6±1.1	6.2±0.02
YX968		591.0±87.5	283.8±50.6	740.1±302.7

XZ9002[b]	650.0±70.0[b]	350.0±70.0[b]	1,093.0±73.5

[a] IC_{50} was determined using Prism [log(inhibitor) vs. response (three parameters) and least-square fit]. Each value is the average of two independent assays ± standard deviation.
[b] Data from Xiao et al.[1]

Table S2. The abundance changes of core subunits in the HDAC1/2/3-containing complexes after **YX968** treatment in proteomic studies, related to Figure 4.

MM.1S				MDA-MB-231			
Gene name	**LogFC**	**P-Values**	**Adj.P-Value**	**Gene name**	**LogFC**	**P-Values**	**Adj.P-Value**
RCOR1	-1.2E-01	2.2E-01	8.2E-01	RCOR1	-2.0E-02	4.4E-01	8.6E-01
RCOR3	-5.2E-01	1.2E-03	4.1E-01	RCOR3	-1.8E-02	7.0E-01	9.3E-01
MTA1	3.4E-02	6.3E-01	8.8E-01	MTA1	6.8E-03	8.8E-01	9.7E-01
MTA2	-5.5E-02	1.8E-01	8.2E-01	MTA2	2.2E-02	3.7E-01	8.2E-01
SIN3A	2.8E-02	7.1E-01	9.2E-01	MTA3	-1.5E-02	7.7E-01	9.5E-01
MIDAS	-4.7E-01	1.5E-01	8.2E-01	SIN3A	-4.4E-02	1.5E-01	7.0E-01
DNTTIP1	-1.5E-01	8.4E-01	9.5E-01	SIN3B	-7.4E-03	8.3E-01	9.7E-01
DNTTIP2	3.0E-03	9.4E-01	9.8E-01	MIDEAS	8.6E-02	3.3E-01	8.1E-01
MIER1	-5.1E-01	8.7E-03	4.1E-01	DNTTIP1	-5.1E-03	9.1E-01	9.8E-01
MIER3	-9.3E-01	1.5E-03	4.3E-01	DNTTIP2	2.6E-04	1.0E+00	1.0E+00
GPS2	-4.9E-01	4.6E-02	8.2E-01	MIER1	-4.6E-02	2.5E-01	7.7E-01
TBL1X	1.1E-01	6.7E-02	8.2E-01	MIER2	-7.8E-02	4.8E-01	8.7E-01
TBL1XR1	9.1E-02	4.0E-01	8.2E-01	GPS2	-1.4E-01	3.7E-02	5.9E-01
NCOR1	-6.9E-01	5.7E-05	1.2E-01	TBL1XR1	2.5E-03	9.2E-01	9.8E-01
SAP130	-1.9E-01	6.0E-02	8.2E-01	NCOR1	-4.7E-01	2.9E-07	2.1E-03
SUDS3	1.7E-01	1.6E-01	8.2E-01	NCOR2	-2.3E-01	1.6E-03	3.7E-01
ARID4B	1.4E-01	2.4E-01	8.2E-01	SAP30	-1.3E-02	8.0E-01	9.6E-01
RBBP4	-2.0E-02	4.5E-01	8.4E-01	SUDS3	-2.8E-02	3.9E-01	8.4E-01
RBBP7	1.2E-01	2.2E-01	8.2E-01	ARID4B	-6.3E-03	9.0E-01	9.8E-01
CHD4	5.0E-02	2.5E-01	8.2E-01	RBBP4	-1.8E-02	5.0E-01	8.8E-01
MBD2	1.3E-01	1.3E-01	8.2E-01	RBBP7	-7.1E-03	8.7E-01	9.7E-01
MBD3	1.1E-01	4.0E-01	8.3E-01	CHD3	-2.5E-02	6.3E-01	9.1E-01
GATAD2A	-9.0E-02	2.1E-01	8.2E-01	CHD4	1.5E-01	1.7E-01	7.0E-01
GATAD2B	8.0E-02	4.1E-01	8.3E-01	MBD2	7.1E-02	2.2E-01	7.5E-01

KDM1A	-2.4E-01	4.0E-02	8.2E-01	MBD3	5.4E-02	2.3E-01	7.6E-01
BAHD1	-2.7E-01	1.8E-01	8.2E-01	GATAD2A	2.8E-02	4.9E-01	8.8E-01
RERE	4.1E-01	5.2E-01	8.4E-01	GATAD2B	5.5E-02	1.7E-01	7.0E-01
ATN1	1.0E-01	4.9E-01	8.4E-01	KDM1A	7.3E-03	7.4E-01	9.5E-01
				RERE	-5.4E-02	4.2E-01	8.5E-01
				ATN1	-2.0E-02	7.5E-01	9.5E-01

Figure S1

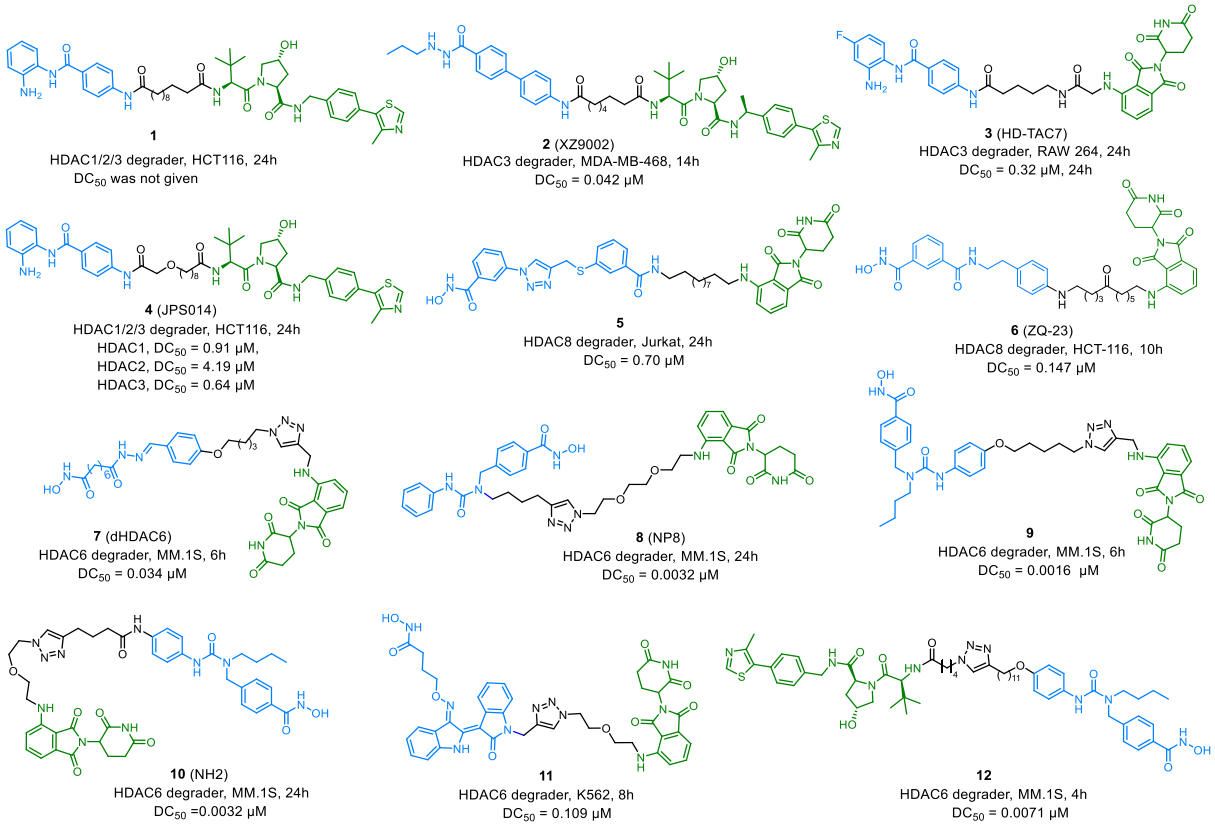

Figure S1. Representative HDAC targeting PROTACs, related to Introduction and Figure 1

Sources: **1**,[2] **2**,[1] **3**,[3] **4**,[4] **5**, **6**,[5] **7**,[6] **8**,[7] **9**,[8] **10**,[9] **11**,[10] and **12**.[11]

Figure S2

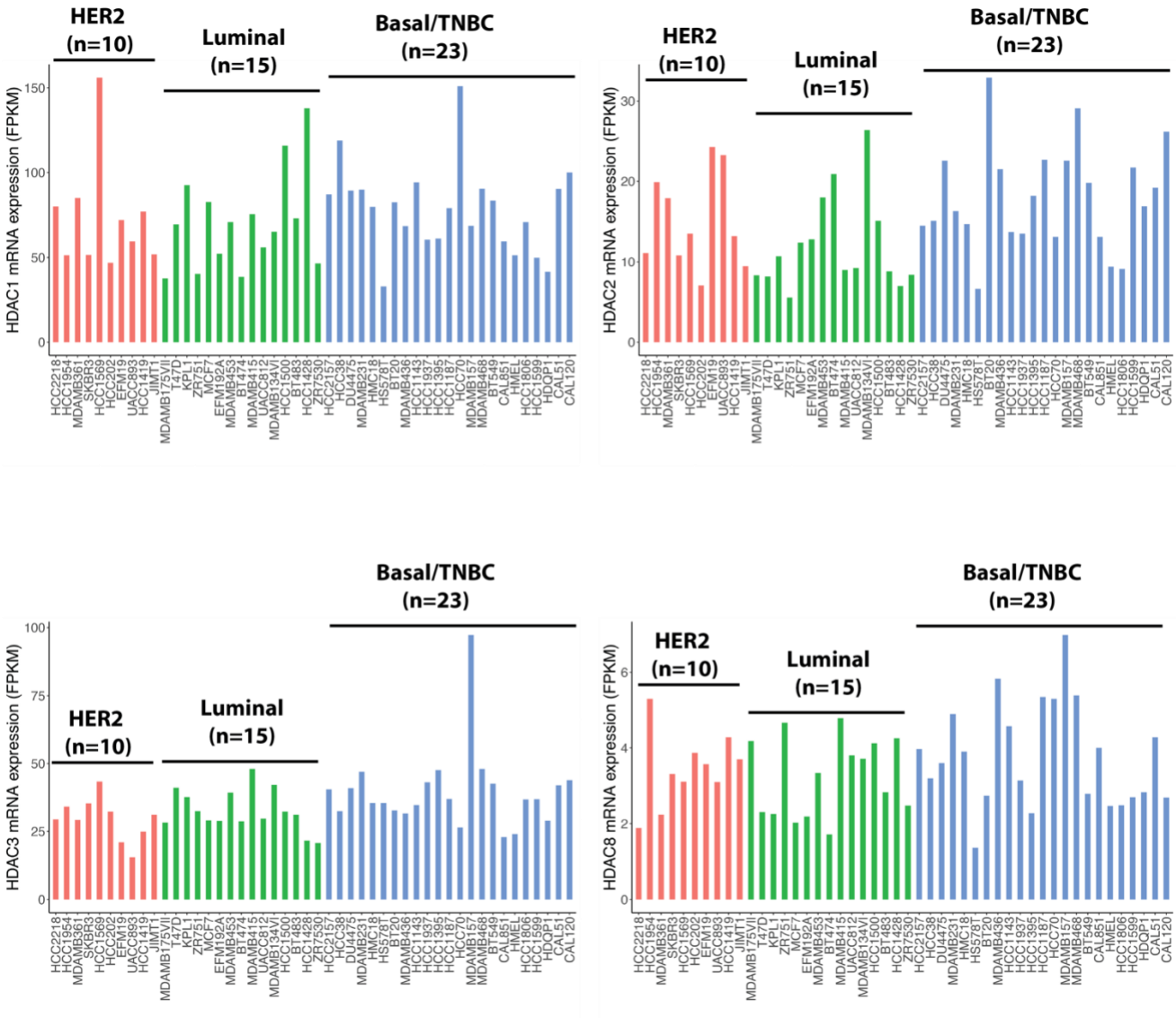

Figure S2. mRNA levels in BC cell lines, related to Figures 1 to 3

The mRNA data are obtained from CCLE (Cancer Cell Line Encyclopedia) and plotted for a panel of BC cell lines. The cell lines are clustered according to breast cancer subtypes. Her2, HER2-enriched, Luminal, ER+, TNBC, triple-negative breast cancer.

Figure S3

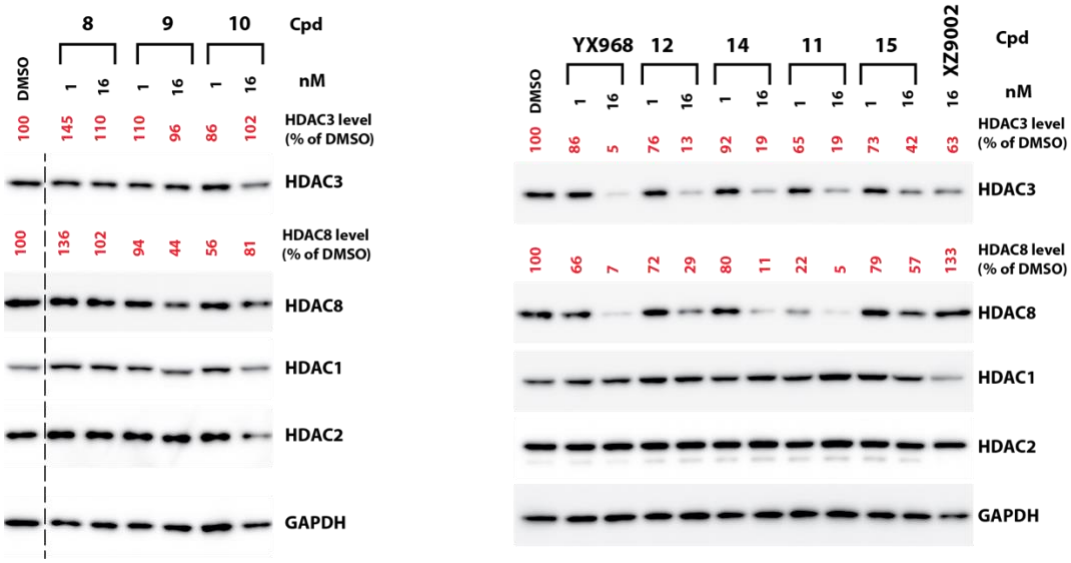

Figure S3. Representative data of Western blotting validation of HDAC3 and HDAC8 degradation. Related to Figures 1 and 2

MDA-MB-231 cells were treated with the indicated compounds at the specified concentrations for 8 h. The cell lysates were subjected to Western blotting using antibodies against the indicated proteins. Protein band intensities were quantified using ImageJ and normalized against that of GAPDH. Relative levels of HDAC3 and HDAC8 after treatment are shown.

Figure S4

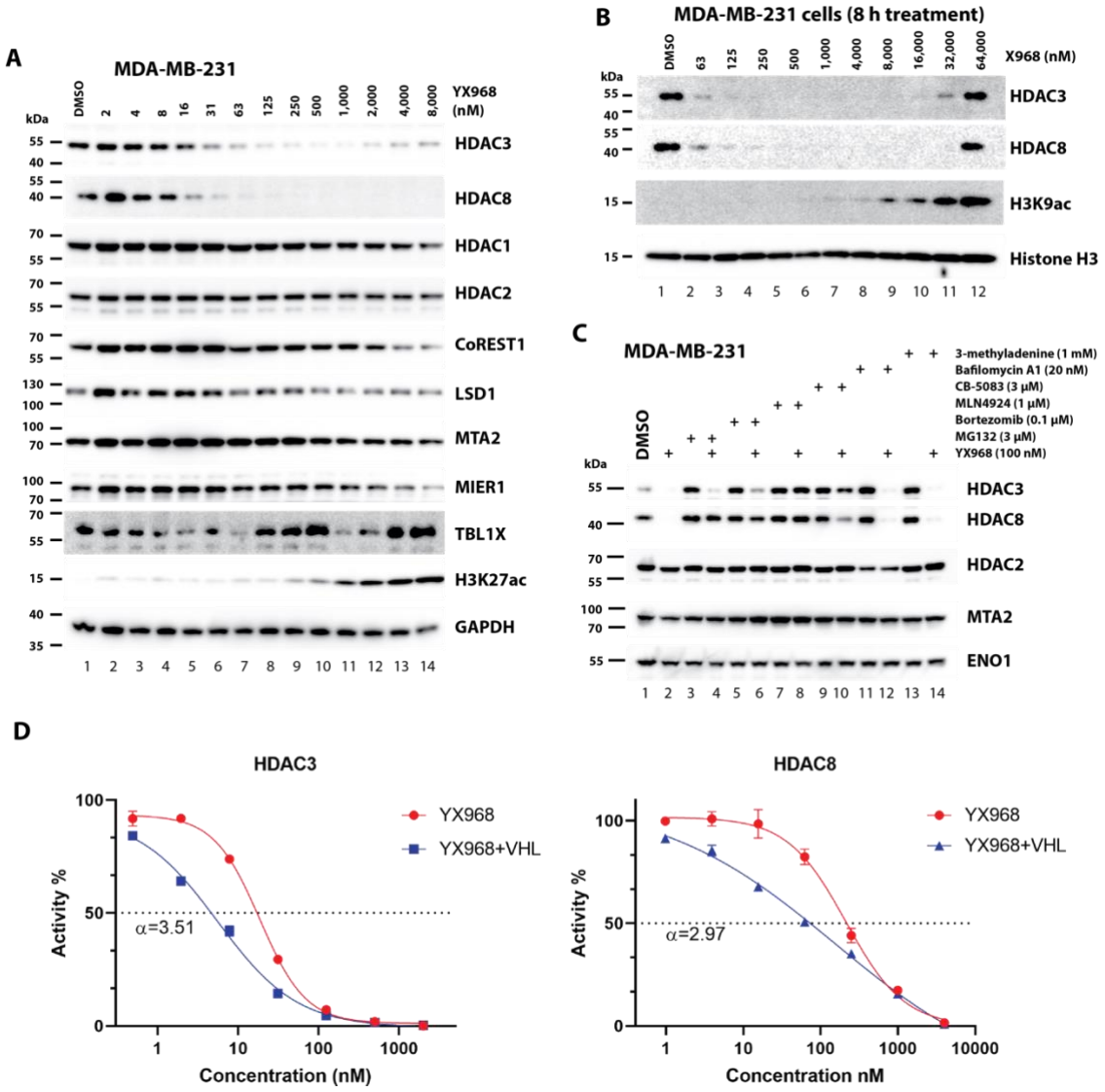

Figure S4. Dose-response and mechanism of target degradation by YX968, related to Figures 2 and 3

(A and B) MDA-MB-231 cells were treated **YX968** at the indicated concentrations for 8h. The lysates of treated cells were subjected to Western blotting using antibodies against the indicated proteins.

(C) MDA-MB-231 cells were pretreated with MG132, bortezomib, MLN4924, CB-5083, bafilomycin A1, or 3-mrthyladenine at the specified concentrations for 2 h. **YX968** was then added, and cells were allowed to grow for 6 more hours. The cells were lysed, and lysates were subjected to Western blotting using antibodies against the indicated proteins.

(D) In vitro HDAC I/II-Glo assay was performed with recombinant HDAC3/NCOR2 proteins or HDAC8 protein with or without the VHL complex. Inhibitory cooperativity (α) was calculated based on IC_{50} (**YX968**)/IC_{50} (**YX968**+VHL). Error bars are mean ± SEM from three independent replicates.

Figure S5

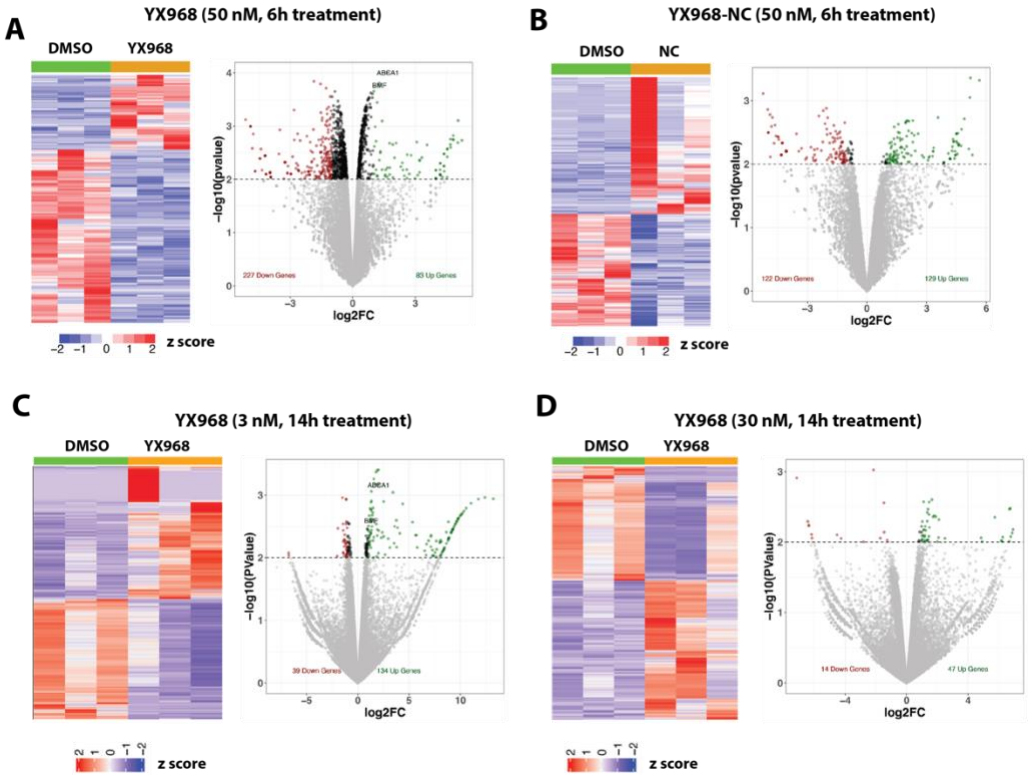

Figure S5. RNA-seq analysis in MDA-MB-231 cells treated with YX968, related to Figure 5.

(A) Heatmap analysis of gene expression data (triplicates from cells treated with DMSO and 50 nM **YX968** for 6h) and a volcano plot of DEGs.

(B) Heatmap analysis of gene expression data (triplicates from cells treated with DMSO and 50 nM **YX968-NC** for 6h) and a volcano plot of DEGs.

(C) Heatmap analysis of gene expression data (triplicates from cells treated with DMSO and 3 nM **YX968** for 14h) and a volcano plot of DEGs.

(D) Heatmap analysis of gene expression data (triplicates from cells treated with DMSO and 30 nM **YX968** for 14h) and a volcano plot of DEGs.

Figure S6

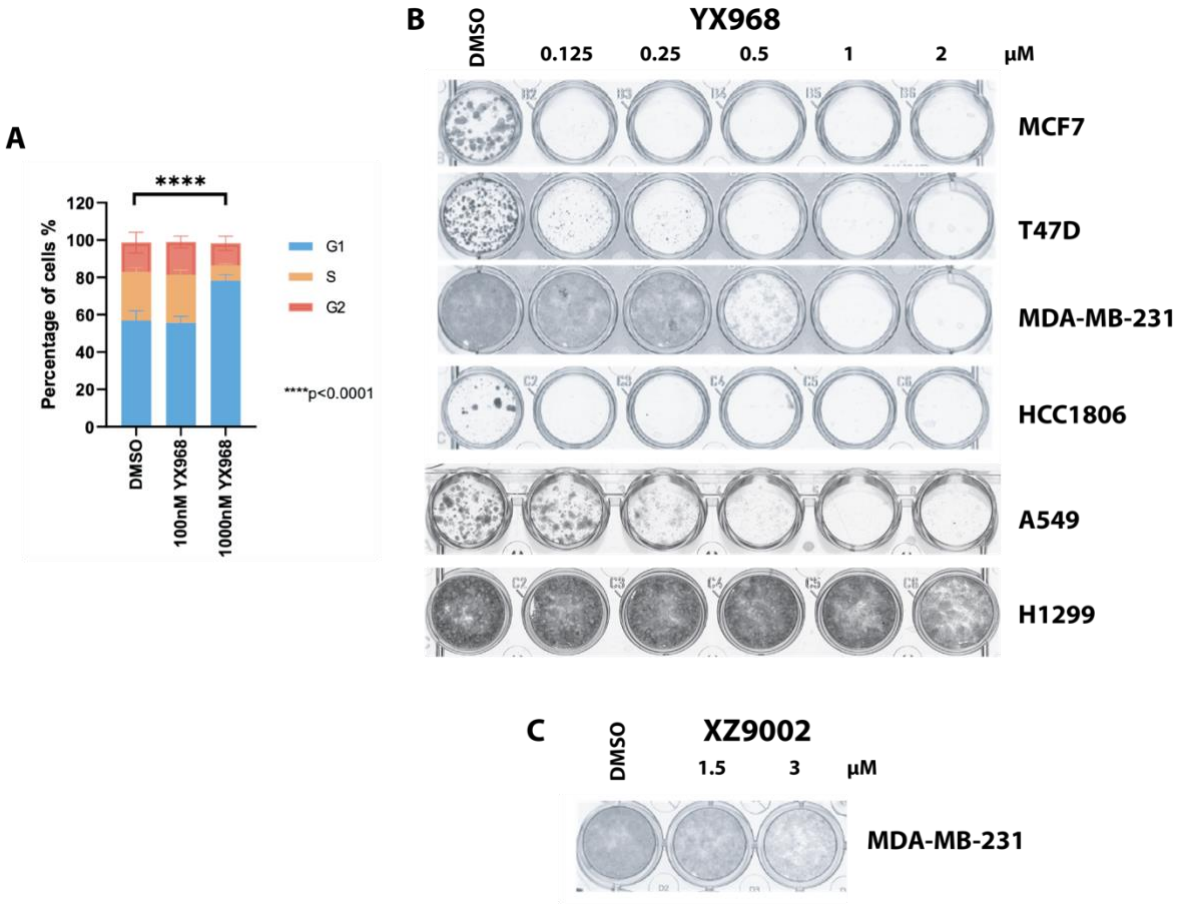

Figure S6. Effects of YX968 on cell cycle and clonogenic growth of breast and lung cancer cell lines, related to Figure 6.

(A) Effects of **YX968** on cell cycle profiles. MDA-MB-231 cells were treated for 24h and subjected to flow cytometry analysis. The P value was calculated based on two-way ANOVA.

(B and C) The indicated cell lines were exposed to DMSO, **YX968** (A) and **XZ9002** (B) at the indicated concentrations. Colonies were fixed and stained after treatment.

References

1. Xiao, Y., Wang, J., Zhao, L.Y., Chen, X., Zheng, G., Zhang, X., and Liao, D. (2020). Discovery of histone deacetylase 3 (HDAC3)-specific PROTACs. Chem Commun (Camb) *56*, 9866-9869. 10.1039/d0cc03243c.
2. Smalley, J.P., Adams, G.E., Millard, C.J., Song, Y., Norris, J.K.S., Schwabe, J.W.R., Cowley, S.M., and Hodgkinson, J.T. (2020). PROTAC-mediated degradation of class I histone deacetylase enzymes in corepressor complexes. Chem Commun (Camb) *56*, 4476-4479. 10.1039/d0cc01485k.
3. Cao, F., de Weerd, S., Chen, D., Zwinderman, M.R.H., van der Wouden, P.E., and Dekker, F.J. (2020). Induced protein degradation of histone deacetylases 3 (HDAC3) by proteolysis targeting chimera (PROTAC). Eur J Med Chem *208*, 112800. 10.1016/j.ejmech.2020.112800.
4. Smalley, J.P., Baker, I.M., Pytel, W.A., Lin, L.Y., Bowman, K.J., Schwabe, J.W.R., Cowley, S.M., and Hodgkinson, J.T. (2022). Optimization of Class I Histone Deacetylase PROTACs Reveals that HDAC1/2 Degradation is Critical to Induce Apoptosis and Cell Arrest in Cancer Cells. J Med Chem *65*, 5642-5659. 10.1021/acs.jmedchem.1c02179.
5. Sun, Z., Deng, B., Yang, Z., Mai, R., Huang, J., Ma, Z., Chen, T., and Chen, J. (2022). Discovery of pomalidomide-based PROTACs for selective degradation of histone deacetylase 8. Eur J Med Chem *239*, 114544. 10.1016/j.ejmech.2022.114544.
6. Yang, K., Song, Y., Xie, H., Wu, H., Wu, Y.T., Leisten, E.D., and Tang, W. (2018). Development of the first small molecule histone deacetylase 6 (HDAC6) degraders. Bioorg Med Chem Lett *28*, 2493-2497. 10.1016/j.bmcl.2018.05.057.
7. An, Z., Lv, W., Su, S., Wu, W., and Rao, Y. (2019). Developing potent PROTACs tools for selective degradation of HDAC6 protein. Protein Cell *10*, 606-609. 10.1007/s13238-018-0602-z.
8. Wu, H., Yang, K., Zhang, Z., Leisten, E., Li, Z., Xie, H., Liu, J., Smith, K.A., Novakova, Z., Barinka, C., and Tang, W. (2019). Development of Multi-Functional Histone Deacetylase 6 Degraders with Potent Anti-Myeloma Activity. J Med Chem. 10.1021/acs.jmedchem.9b00516.
9. Yang, H., Lv, W., He, M., Deng, H., Li, H., Wu, W., and Rao, Y. (2019). Plasticity in designing PROTACs for selective and potent degradation of HDAC6. Chem Commun (Camb) *55*, 14848-14851. 10.1039/c9cc08509b.
10. Cao, Z., Gu, Z., Lin, S., Chen, D., Wang, J., Zhao, Y., Li, Y., Liu, T., Li, Y., Wang, Y., et al. (2021). Attenuation of NLRP3 Inflammasome Activation by Indirubin-Derived PROTAC Targeting HDAC6. ACS Chem Biol. 10.1021/acschembio.1c00681.
11. Yang, K., Wu, H., Zhang, Z., Leisten, E.D., Nie, X., Liu, B., Wen, Z., Zhang, J., Cunningham, M.D., and Tang, W. (2020). Development of Selective Histone Deacetylase 6 (HDAC6) Degraders Recruiting Von Hippel-Lindau (VHL) E3 Ubiquitin Ligase. ACS Med Chem Lett *11*, 575-581. 10.1021/acsmedchemlett.0c00046.